



Effect of silica on the thermal behaviour and ionic conductivity of mixed salt solid acid composites



Norsyahida Mohammad^a, Abu Bakar Mohamad^{a, b}, Abdul Amir H. Kadhum^{a, b}, Kee Shyuan Loh^{a, *}

^a Fuel Cell Institute, Universiti Kebangsaan Malaysia, 43600, UKM, Bangi, Selangor, Malaysia

^b Department of Chemical and Process Engineering, Universiti Kebangsaan Malaysia, 43600, UKM, Bangi, Selangor, Malaysia

ARTICLE INFO

Article history:

Received 13 June 2016

Received in revised form

17 August 2016

Accepted 19 August 2016

Available online 21 August 2016

Keywords:

Solid acid composite

Silica

Thermal properties

Ionic conductivity

ABSTRACT

The effect of adding silica (SiO₂) to a mixed-salt solid acid composite, CsH₂PO₄/NaH₂PO₄, was studied via conductivity measurements, thermal analyses and X-ray diffraction. The conductivity value of the composites ranged from 1.1×10^{-4} S cm⁻¹ to 7.6×10^{-3} S cm⁻¹ for temperatures from 210 °C to 250 °C, respectively. Adding NaH₂PO₄ to the composite reduced the conductivity value at 230 °C due to the decomposition of NaH₂PO₄, which initiated at 210 °C. Dehydration of CsH₂PO₄ was evident at 230 °C and 270 °C, while the superprotonic phase transition was not observed. Dehydration was detected for NaH₂PO₄ at temperatures above 210 °C, but a thermally stable composite was produced by mixing it with CsH₂PO₄ and SiO₂. An X-ray diffraction analysis confirmed the existence of solid acid solutions for the composites consisting of NaH₂PO₄:CsH₂PO₄ and SiO₂:CsH₂PO₄ in molar ratios of 1:10 to 3:10. The presence of SiO₂ partially obstructed the dehydration of the composite, as the diffraction intensity of the dehydration by-product Cs₂H₂P₂O₇ decreased at the end of the thermal treatment.

© 2016 Elsevier B.V. All rights reserved.

1. Introduction

Solid acids are proton-conducting materials with the general chemical formula of M_aH_b(XO₄)_c, where M is a monovalent or divalent metal cation, XO₄ is a tetrahedral oxy-anion, and a, b, and c are integers [1]. Solid acids, such as CsH₂PO₄, RbH₂PO₄ and CsHSO₄, are among the most well-characterized and promising solid acids for fuel cell applications due to their high proton conductivity, also known as superprotonic conductivity, whereby the conductivity increases by 2–3 orders of magnitude when the material is heated to high temperatures. Generally, solid acids are utilized as the electrolyte and mixed into the electrocatalyst layers of solid acid fuel cells operating at temperatures between 100 °C and 250 °C. The high operating temperature range eliminates the issues of catalyst inefficiency and intolerance to carbon monoxide (CO) associated with fuel cells working at low temperatures such as proton exchange membrane fuel cells (PEMFCs).

Recent studies have been moving towards synthesizing and

characterizing solid acid composites that are mixed-salt solid acids and composites with oxides and polymers. Mixed solid acids, also known as binary solid acid composites, exhibit properties superior to those of single-salt solid acids such as wider temperature ranges of superprotonic conductivity and higher protonic conductivity at lower temperatures due to reduced activation enthalpy [2–5]. Partial substitution with larger cations or tetrahedral oxy-anions increases the hydrostatic pressure and induces superprotonic behaviour in solid acids [5].

The addition of hygroscopic oxides, such as silica (SiO₂), zirconia (ZrO₂), titania (TiO₂) and alumina (Al₂O₃), produces solid acid composites that are more robust and less brittle [1,5]. These properties facilitate the fabrication of an electrolyte and electrode assembly for fuel cell construction. Furthermore, adding these hygroscopic oxides increases proton conductivity over wider temperature ranges and at lower vapour pressures in comparison to the pure solid acid [6,7]. These oxides enhance the thermal stability of solid acid composites because filling the alumina matrix with the solid acids caesium hydrogen sulphate, CsHSO₄ (CHS) and caesium dihydrogen phosphate, CsH₂PO₄ (CDP) results in invariant conductivity values during heating and cooling cycles compared to the pure solid acids [5,8]. High temperature thermoplastics, such as perfluorinated polymers, polybenzimidazole (PBI), fluoroelastomers

* Corresponding author.

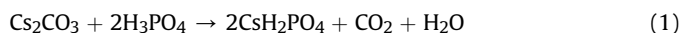
E-mail addresses: norsyahida_mohammad@yahoo.co.uk (N. Mohammad), drab@ukm.edu.my (A.B. Mohamad), amir@ukm.edu.my (A.A.H. Kadhum), ksloh@ukm.edu.my (K.S. Loh).

and polytetrafluoroethylene (PTFE), can also be added as binders to produce more flexible, less brittle solid acid composites [9].

Compared with other solid acids, CDP has the highest conductivity value ($2.2 \times 10^{-2} \text{ S cm}^{-1}$ at 240°C) and is stable in hydrogen-rich surroundings [10–13]. A recent study by Martsinkevich and Ponomareva [3] examined the effects of mixing CDP with sodium dihydrogen phosphate, NaH_2PO_4 (SDP), and found that the mixed salt solid acid $\text{Cs}_{1-x}\text{Na}_x\text{H}_2\text{PO}_4$, with an x value up to 0.2, increases the low temperature conductivity of CDP by up to 2 orders of magnitude. The authors found, however, that SDP alone does not exhibit superprotonic conductivity and is known for dehydration and a low melting point [3]. In this study, we investigate the effect of adding a hygroscopic oxide, SiO_2 , to the mixed-salt solid acid CDP/SDP via thermal and structural characterization techniques. The SDP:CDP ratios were also varied to identify the effects of adding SDP on the properties of the solid acid composite $\text{CsH}_2\text{PO}_4/\text{NaH}_2\text{PO}_4/\text{SiO}_2$. Thus far, we have not studied the effects of adding other types of additives or hygroscopic oxides.

2. Materials and methods

CDP was synthesized by aqueous mixing of stoichiometric amounts of caesium carbonate, Cs_2CO_3 (ReagentPlus[®], $\geq 99\%$ Sigma Aldrich, MO, USA) and phosphoric acid, H_3PO_4 ($\geq 85 \text{ wt\%}$ in H_2O , Sigma Aldrich, MO, USA) according to the following reaction:



Cs_2CO_3 was measured as required and dissolved in distilled water. A surfactant powder, cetyltrimethylammonium bromide (CTAB) (BioXtra[®], $\geq 99\%$ Sigma Aldrich, MO, USA), was dissolved in ethanol separately and added to the Cs_2CO_3 solution to reduce the water surface tension and assist particle dispersion. Using surfactants such as CTAB and Pluronic F-68 solution in solid acid synthesis was studied by Hosseini et al. [14], who found that the CTAB cationic surfactant assists proton movement within the solid acid material. The Cs_2CO_3 mixture was then stirred for 10 min until a clear solution was produced. Next, phosphoric acid was added drop-wise with continuous stirring for another 10 min. Excessive acetone was added to the mixture to induce precipitation. The mixture was stirred for another 30 min, followed by filtration to separate polycrystalline CDP from the solution. The white precipitate CDP was dried at 130°C for 24 h to eliminate absorbed water due to the hygroscopic property of the solid acid prior to grinding the precipitate to produce powdered CDP.

Solid acid composites, $\text{CsH}_2\text{PO}_4/\text{NaH}_2\text{PO}_4/\text{SiO}_2$, were synthesized by mixing CDP, NaH_2PO_4 (ReagentPlus[®], $\geq 99\%$ Sigma Aldrich, MO, USA) and SiO_2 (purum p.a. powder, Sigma Aldrich, MO, USA, $63 \mu\text{m}$ particle size) according to the ratios in Table 1. The dry mixing method was utilized by Martsinkevich and Ponomareva [3] to synthesize the double salts $\text{Cs}_{1-x}\text{Na}_x\text{H}_2\text{PO}_4$ with x values of 0–0.9. The authors found that both aqueous mixing and the dry

mixing method produce solid acid composites with similar structures and thermal properties [3].

Conductivity measurements were conducted via electrochemical impedance spectroscopy (EIS) with a 2-electrode configuration at ambient pressure in air at room temperature and high temperatures between 210°C and 250°C . The solid acid powders were pressed into pellets of 1 mm thickness and 13 mm diameter by uniaxially pressing at 3 tonnes cm^{-2} for 1 min at room temperature, producing solid acid pellets with a surface area of 1.33 cm^2 . The pellets were painted with a silver (Ag) suspension on both sides and then heat treated to cure the Ag layer. This Ag layer enhances the contact of the surfaces with the current collector. The pellet was then sandwiched between two squares of platinum mesh with dimensions of $15 \text{ mm} \times 15 \text{ mm}$ (100 mesh, 99.9% trace metal basis), which acts as the current collector and was placed inside a metal pellet holder with a ceramic lining and connected to an Autolab impedance analyser. The impedance readings were taken within frequency ranges of 1.0×10^{-2} to $1.0 \times 10^6 \text{ Hz}$ and at a 0.01 A current. The measured data were analysed using the Nova software package. The proton conductivity value was determined from the impedance data plotted on the real and imaginary axes, Z' and $-Z''$, respectively, known as a Nyquist plot. The curve was fitted using the equivalent circuit shown in Fig. 1a. The proton conductivity values, σ , for pure CDP and the $\text{CsH}_2\text{PO}_4/\text{NaH}_2\text{PO}_4/\text{SiO}_2$ (CDP/SDP/ SiO_2) composites were calculated using the resistance value, R , and are given by the following equation:

$$\text{Conductivity, } \sigma (\text{S cm}^{-1}) = 1/R(\Omega) / A(\text{cm}^2) / l(\text{cm}) \quad (2)$$

where A is the surface area of the pellet and l is the thickness of the pellet.

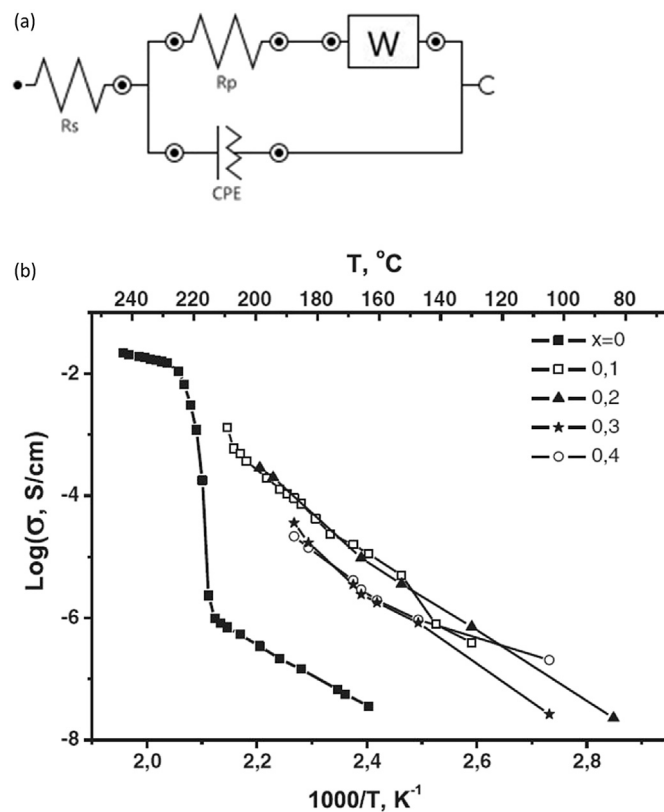


Fig. 1. (a) The equivalent circuit used to analyze the impedance data; (b) Proton conductivity of mixed-salt $\text{Cs}_{1-x}\text{Na}_x\text{H}_2\text{PO}_4$ plotted during cooling cycle, $1-2^\circ\text{C min}^{-1}$ in air. Reproduced with permission [3].

Table 1
Molar ratio of solid acid composites synthesized.

| Solid acid sample | $\text{CsH}_2\text{PO}_4/\text{NaH}_2\text{PO}_4/\text{SiO}_2$ molar ratio |
|-------------------|--|
| CDP 11 | 10:1:1 |
| CDP 12 | 10:1:2 |
| CDP 13 | 10:1:3 |
| CDP 21 | 10:2:1 |
| CDP 22 | 10:2:2 |
| CDP 23 | 10:2:3 |
| CDP 31 | 10:3:1 |
| CDP 32 | 10:3:2 |
| CDP 33 | 10:3:3 |

The thermal stability of the solid acid materials was measured via differential scanning calorimetry (DSC) and thermogravimetric analysis (TGA). The DSC measurements display endothermic or exothermic peaks during heating of the solid acid, which are usually related to either dehydration or phase transitions of the solid acid. Solid acid decomposition is identified by measuring the mass loss as a function of temperature via TGA analysis. Both DSC and TGA measurements were run simultaneously using an STA 449 F3 Netzsch simultaneous TGA-DSC between 30 °C and 600 °C with a heating rate of 5 °C min⁻¹ under nitrogen flow.

X-ray diffraction (XRD) measurements were conducted using a D8 Advance diffractometer (Bruker AXS Germany) with CuK α radiation at a wavelength of 0.15406 nm, a 0.025° step size and a heating rate of 0.2 °C sec⁻¹. Measurements were conducted within a standard 2 θ range from 10° to 60° at ambient pressure in air at room temperature, 200 °C, 225 °C, 235 °C and 245 °C. This measurement is essential for the identification of the phases and crystal orientations of solid acids. The occurrence of the superprotonic phase transition is observed when a change in the solid acid phase occurs at temperatures between 100 °C and 250 °C accompanied by an immediate increase in the conductivity value.

3. Results and discussion

The conductivities of the solid acid CDP and its composites are presented in Table 2. We observed a CDP conductivity value of 1.9×10^{-2} S cm⁻¹ at 230 °C, which is comparable to the value determined by Haile et al. [10]. SDP is known for its low conductivity and its absence of superprotonic behaviour at high temperatures. The conductivity of SDP was measured to be 2.2×10^{-4} S cm⁻¹ at 230 °C.

A study of the conductivity of Cs_{1-x}Na_xH₂PO₄ for x values of 0–0.3 at lower temperatures between 100 °C and 210 °C, conducted by Martsinkevich and Ponomareva [3], indicated that the composites show higher conductivity than pure CDP, as shown in Fig. 1b. This is due to the difference in the sizes of the Na⁺ and Cs⁺ cations within the CDP composite, which initiates disorder within the composite's structure at temperatures lower than the superprotonic temperature of CDP, i.e., 230 °C [3]. Similarly, Otomo et al. [6] found that the CDP/SiO₂ composite for a silica mole fraction of 0.33 exhibited a higher conductivity value than that of pure CDP at temperatures lower than 230 °C. This higher conductivity was attributed to defects at the interface of both components [6]. The authors also found that the properties of the silica support, such as the hydrophilicity and surface area, affect the conductivity of the CDP/SiO₂ composite [6], but these factors were not examined in the present study. Ponomareva and Shutova [7] claimed that a CDP

composite with an acidic-center-modified-SiO₂ mole fraction of 0.3 produced a higher proton conductivity of approximately 10^{-3} to 10^{-2} S cm⁻¹ over a broader temperature range of 130 °C–250 °C in comparison to that of pure CDP. From these findings, it could be deduced that adding SiO₂ increases the conductivity of the solid acid composite.

Our measurements indicated that the conductivity value of the composite ranges from 1.1×10^{-4} S cm⁻¹ to 7.6×10^{-3} S cm⁻¹ as SiO₂ is added to the CDP/SDP, with some conductivity values higher than the conductivity of the CDP/SDP mixed salt obtained by Martsinkevich and Ponomareva [3].

We analysed the thermal stability of the solid acids CDP and SDP and the CDP/SDP/SiO₂ composites via DSC and TGA measurements to identify the occurrence of dehydration and decomposition when the materials were heated to high temperatures. The DSC measurement for CDP in Fig. 2 indicated endothermic heat flows at 230 °C and 270 °C, similar to the findings by Rashkovich et al. as presented by Boysen et al. [15]. However, this DSC measurement did not trace the endothermic peak at 149 °C reported by Metcalfe and Clark [16]. Metcalfe and Clark [16] found that CDP powder undergoes two endothermic transitions, a quasi-irreversible transition at 149 °C and a reversible transition at 230 °C with enthalpies of 1.071 kJ mol⁻¹ and 7.615 kJ mol⁻¹, respectively [16]. The TGA measurement (Fig. 2) showed that negligible weight loss due to the dehydration of water molecules at the surface of the CDP crystals occurred up to 230 °C. Subsequently, there was a significant mass reduction, denoted by the endothermic peaks of our DSC measurement, indicating decomposition of CDP, which produced Cs₂H₂P₂O₇ and CsPO₃ at 230 °C and 270 °C, respectively.

SDP undergoes dehydration at several temperatures between 60 °C and 350 °C [17], as evidenced by the endothermic peaks in Fig. 3. The dehydration at 60 °C was assumed to occur because of water molecules present on the surface of the solid acid crystals due to their hygroscopic property. The TGA measurements for SDP (Fig. 3) indicated that SDP undergoes a two-stage dehydration. The first stage occurred at 210 °C with a weight loss of 8%, and the second stage was dehydration at 340 °C with a 15% overall weight loss. This result is in agreement with the findings by Li and Tang [18] that SDP decomposes when heated, producing disodium dihydrogen pyrophosphate, Na₂H₂P₂O₇, at 210 °C with a 7.5% weight loss, followed by a second stage of decomposition between 223 °C and 352 °C, producing NaPO₃ with a 14.9% overall weight loss. An earlier study by Gupta et al. [19] claimed that SDP undergoes dehydration at the slightly lower temperatures of 169 °C and 240 °C. This is probably due to the different heating rates imposed on the material during thermal analyses. It has been found that different products are produced when SDP is heated at

Table 2
Conductivity values of CDP and its composites.

| Solid acids | Highest conductivity value, σ (S cm ⁻¹) | Temperature during conductivity measurement (°C) |
|--|--|--|
| CDP [10] | 2.2×10^{-2} | 240 |
| CDP (pure) | 1.9×10^{-2} | 230 |
| SDP (pure) | 2.2×10^{-4} | 230 |
| 0.67 CsH ₂ PO ₄ /0.33SiO ₂ [6] | 1.65×10^{-5} | 225 |
| Cs _{0.8} Na _{0.2} H ₂ PO ₄ [3] | 3.2×10^{-4} | 200 |
| CDP11 | 6.6×10^{-4} | 210 |
| CDP12 | 1.3×10^{-4} | 230 |
| CDP13 | 3.4×10^{-3} | 250 |
| CDP21 | 7.6×10^{-3} | 250 |
| CDP22 | 1.1×10^{-4} | 210 |
| CDP23 | 2.8×10^{-3} | 230 |
| CDP31 | 4.0×10^{-4} | 230 |
| CDP32 | 7.2×10^{-3} | 250 |
| CDP33 | 3.8×10^{-4} | 210 |

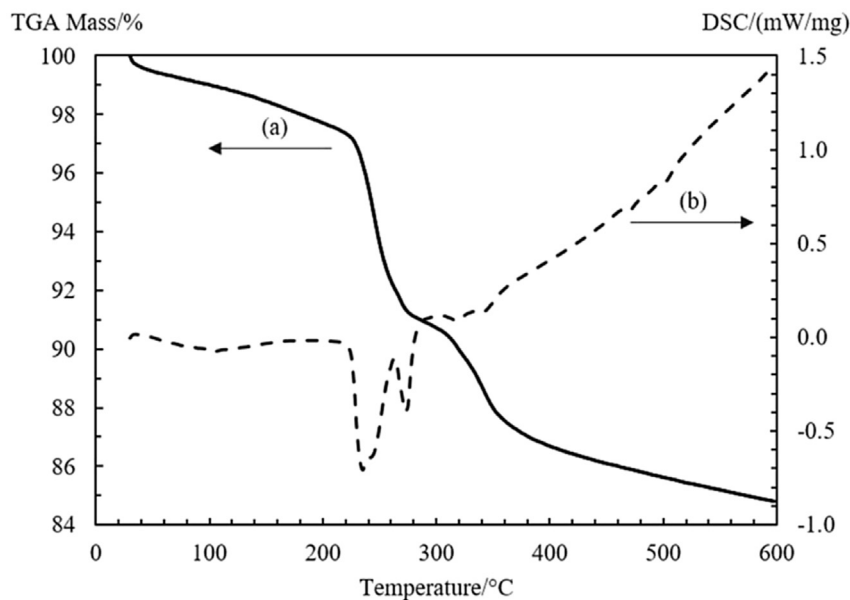


Fig. 2. Thermal analyses via (a) TGA and (b) DSC for CDP.

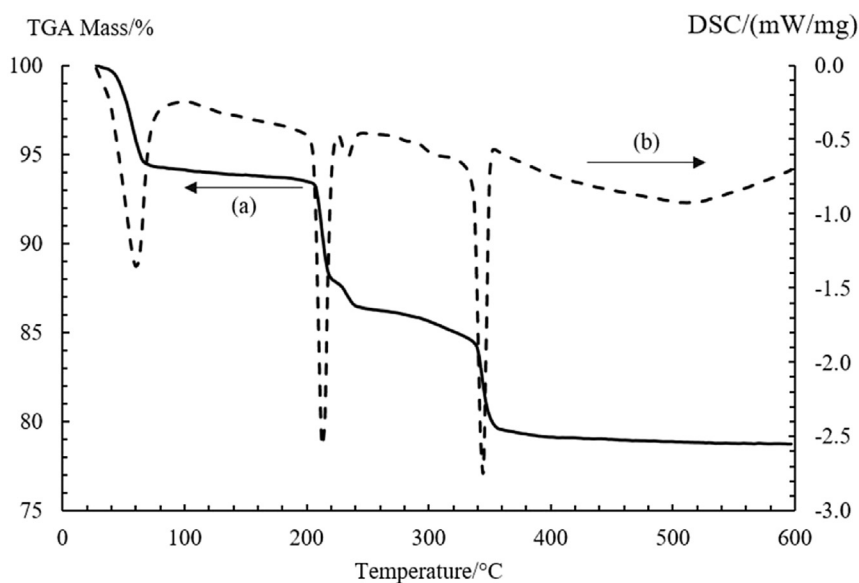


Fig. 3. Thermal analyses via (a) TGA and (b) DSC for SDP. Reproduced with permission [17].

different heating rates [20]. These findings suggest that SDP is less stable than CDP at high temperatures, with decomposition occurring at 210 °C.

DSC measurements for the CDP/SDP/SiO₂ composites revealed that dehydration occurs at temperatures similar to that for pure SDP. Furthermore, ratios of SDP:CDP and SiO₂:CDP varying from 1:10 to 3:10 did not have a significant impact on the thermal behaviour of the composites, as observed in Fig. 4 and Fig. 5. Assuming that the reduction of mass prior to 100 °C is due to water molecules present on the surface of the solid acids, which are hygroscopic in nature, we calculate the weight loss of the solid acids when heated above 100 °C from the TGA measurements. The thermal stability of the solid acid composite is comparable to that of pure CDP at low temperatures up to 200 °C, as depicted for CDP23 (CDP:SDP:SiO₂ molar ratio of 10:2:3) in Fig. 6,

where only a 3% weight loss was detected, indicating a thermally stable composite.

To identify the occurrence of a phase transition, we conducted X-ray diffraction analyses for the solid acids CDP and SDP and the CDP/SDP/SiO₂ composites. Diffraction spectra for CDP, SDP and the CDP23 composite at room temperature are depicted in Fig. 7a–c, respectively. The XRD spectra obtained for CDP in Fig. 7a have similar attributes to those of the CDP plots obtained by Ortiz et al. [21] and Boysen et al. [15], as peaks appear at 18°, 19°, 23.5°, 25.5°, 28° and 29°. The plot in Fig. 7c indicates that a different phase was detected for CDP23 than for the single salt solid acids CDP and SDP, shown in Fig. 7a, b. This confirms the findings of Matsinkevich and Ponomareva [3], which suggested that the solid solution Cs_{1-x}Na_xH₂PO₄ exists only for x values of 0–0.3, while further increases in the molar fraction resulted in the individual phase of SDP,

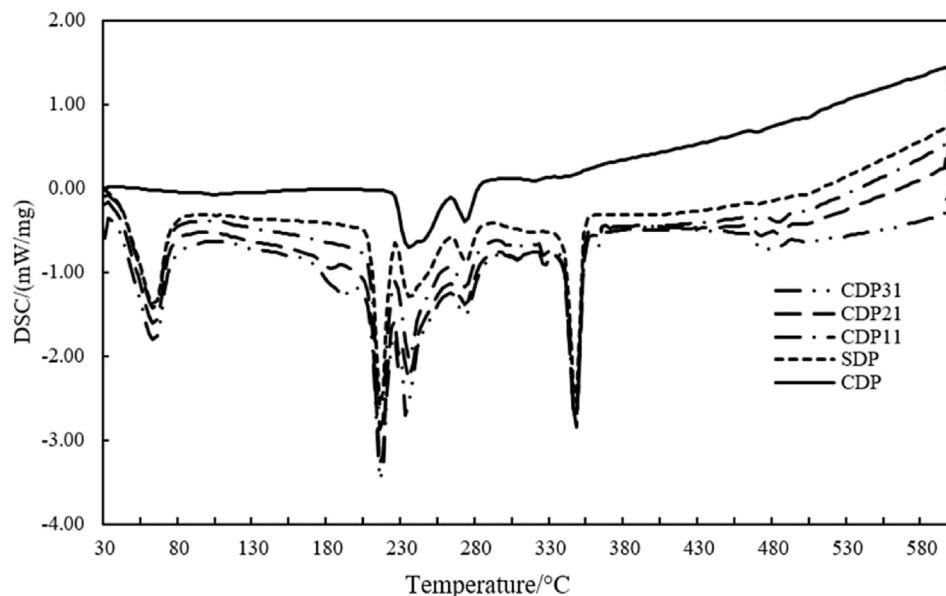


Fig. 4. The DSC curves for CDP/SDP/SiO₂ composites with varied SDP:CDP ratio in comparison with CDP and SDP.

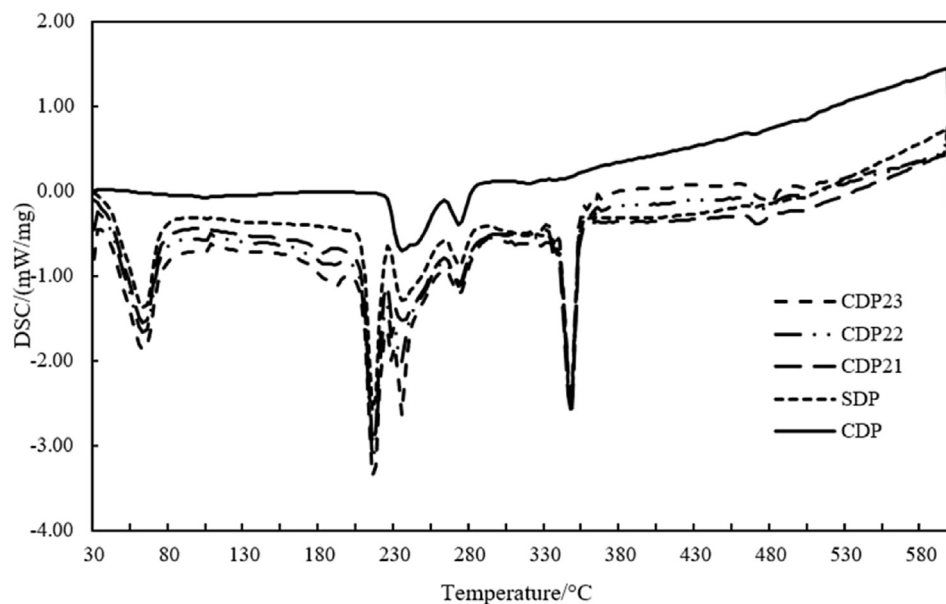


Fig. 5. The DSC curves for CDP/SDP/SiO₂ composites with varied SiO₂:CDP ratio in comparison with CDP and SDP.

identified by the similarity in the diffraction patterns of the composite to those of SDP.

Further XRD measurements were conducted for CDP23 to identify the phase changes of the composite as it was heated to high temperatures. Measurements were conducted on fresh CDP23 powder at room temperature, 200 °C, 225 °C, 235 °C and 245 °C, followed by another measurement after cooling to room temperature. These measurements are plotted in Fig. 8a–f. The diffraction plots at room temperature, 200 °C, 225 °C and 235 °C showed a high intensity peak at approximately 23.6°, which decreased in intensity at 245 °C and stayed at a constant intensity after cooling to room temperature. The peak at approximately 23.6°, corresponding to the Miller indices of (011) for CDP with the monoclinic phase space group $P2_1/m$, is due to several overlapping peaks [6,21]. CDP

exists in the monoclinic phase structure from room temperature up to 245 °C, and it remains in this phase even after cooling to room temperature, as shown in Fig. 8a–f. The intensity of the diffraction peak at 23.6° decreases, however, indicating the partial dehydration of CDP at temperatures between 235 °C and 245 °C, producing Cs₂H₂P₂O₇.

The formation of Cs₂H₂P₂O₇ was confirmed by another persistent peak at 25.2°, marked by asterisks in Fig. 8b–f. This is similar to the findings of Ortiz et al. [21], wherein a peak appeared at 25.2° in each XRD measurement made at room temperature for samples subjected to 1 min of heat treatment at 130 °C, 165 °C, 200 °C, 238 °C and 250 °C. Subsequent thermal analyses by Ortiz et al. [21] confirmed that the peak at 25.2° represents the CDP dehydration product caesium dihydrogen pyrophosphate, Cs₂H₂P₂O₇, as CDP

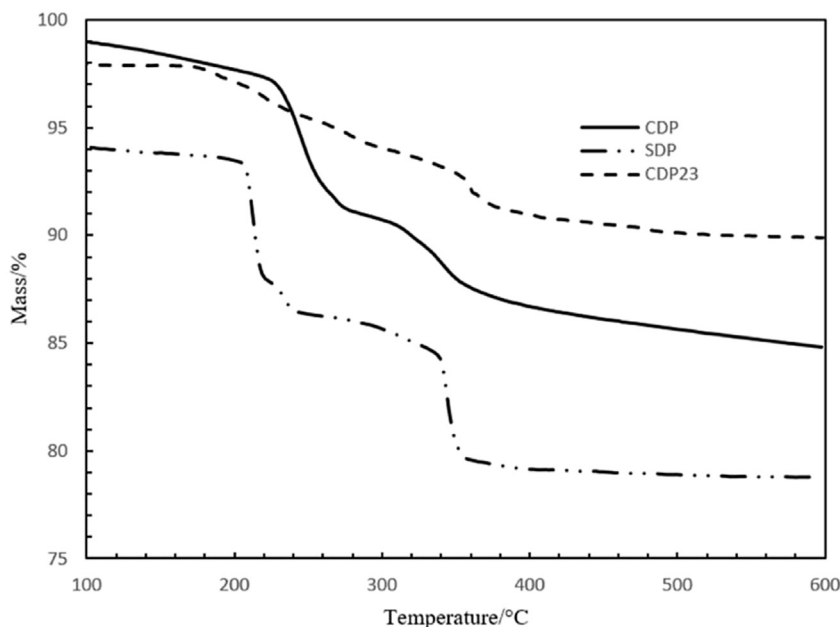


Fig. 6. TGA plots for CDP, SDP and CDP23 composite.

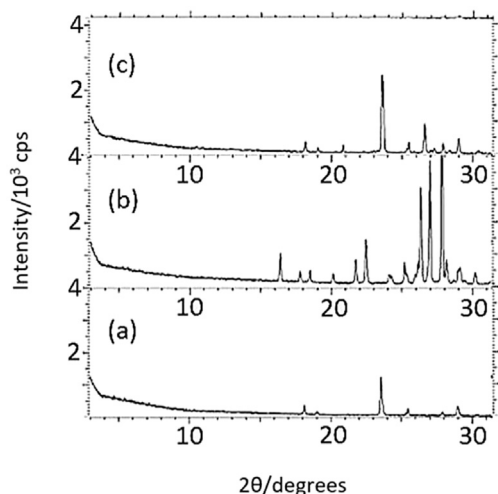


Fig. 7. Comparison between diffraction plots of (a) CDP, (b) SDP and (c) CDP23 composite taken at room temperature.

undergoes dehydration at the surface of the crystal according to the following equation:



Fig. 8f shows that the peak of the dehydration product $\text{Cs}_2\text{H}_2\text{P}_2\text{O}_7$ is slightly lower in intensity than the peak of CDP, in contrast to the findings of Rashkovich and Meteva, as highlighted by Ortiz et al. [21], in which the 25.2° peak of $\text{Cs}_2\text{H}_2\text{P}_2\text{O}_7$ was found to be the highest intensity peak. The low intensity of the $\text{Cs}_2\text{H}_2\text{P}_2\text{O}_7$ peak indicates that the presence of SiO_2 in our solid acid composite partially restrained the dehydration reaction. These findings support an earlier study via the Bond method and a Guinier camera by Bronowska and Pietraszko [22], which revealed that as CDP is heated, the monoclinic phase with lattice parameters $a = 7.917 \text{ \AA}$, $b = 6.495 \text{ \AA}$, $c = 4.850 \text{ \AA}$, and $\beta = 106.71^\circ$ remains up to

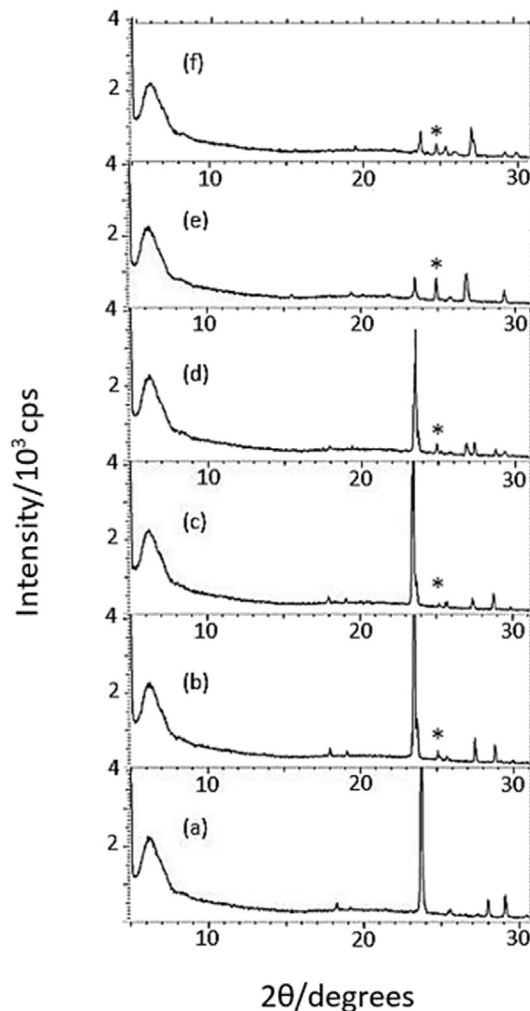


Fig. 8. Compilation of X-ray diffraction plots for CDP23 composite at (a) 25 °C, (b) 200 °C, (c) 225 °C, (d) 235 °C, (e) 245 °C and (f) 25 °C after cooling down of the sample.

decomposition at 247 °C, at which point the orthorhombic phase of $\text{Cs}_2\text{H}_2\text{P}_2\text{O}_7$ is formed with lattice parameters $a = 4.517 \text{ \AA}$, $b = 8.142 \text{ \AA}$, and $c = 11.398 \text{ \AA}$ [22].

Bronowska [23] observed the superprotonic phase transition of CDP from monoclinic to cubic via XRD measurements conducted at 237 °C in a water-saturated environment. This indicates that hydration is essential in enabling observation of the superprotonic transition and preventing the material from dehydrating. The cubic phase related to the superprotonic behaviour of CDP was not observed in our measurements, as the analysis was conducted without humidification.

4. Conclusion

The conductivity values of the CDP/SDP/SiO₂ composites range from $1.1 \times 10^{-4} \text{ S cm}^{-1}$ to $7.6 \times 10^{-3} \text{ S cm}^{-1}$, which are lower than the conductivity of pure CDP at its superprotonic temperature of 230 °C. At lower temperatures between 100 °C and 210 °C, the conductivity values of the composite are higher than the conductivity of the CDP/SDP mixed salt obtained by Martsinkevich and Ponomareva [3].

CDP undergoes dehydration at 230 °C and 270 °C, while SDP dehydration peaks were observed at several temperatures between 210 °C and 350 °C [17], indicating that SDP is thermally unstable at high temperatures. Adding SDP to the composite significantly affects the thermal stability of the composites, and the thermal analyses of the composites showed similar attributes to pure SDP. The thermal analysis conducted on CDP23 at temperatures less than 200 °C detected a 3% overall weight loss, which is comparable to that for pure CDP, demonstrating that adding SiO₂ stabilizes the overall thermal stability.

X-ray diffraction measurements at room temperature confirmed the solid solution of the composite. High temperature XRD measurements for the solid acid composite CDP23 indicated that CDP appears in the monoclinic phase with the space group $P2_1/m$ from room temperature up to 245 °C, as decomposition occurred at the CDP crystal surfaces and the by-product, $\text{Cs}_2\text{H}_2\text{P}_2\text{O}_7$ began to form above this temperature. No phase transition was observed throughout the measurements. At the end of the CDP23 composite thermal treatment, the peak of the dehydration product $\text{Cs}_2\text{H}_2\text{P}_2\text{O}_7$ was found to be slightly lower in intensity than the peak of CDP, indicating that the dehydration reaction is partially obstructed by the presence of SiO₂ within the composite.

Acknowledgements

This work was financially supported by the Ministry of Higher Education, Malaysia (ERGS/1/2012/TK07/UKM/01/1); Universiti Kebangsaan Malaysia (UKM) through University Research Grants (GUP-2016-038 and DIP-2014-002); and the Malaysia Toray Science Foundation (UKM-MTSF-SELFUEL-2-2010).

References

- [1] D.A. Boysen, *Superprotonic Solid Acids: Structure, Properties, and Applications* [Dissertation], California Institute of Technology, 2004.
- [2] S. Gadzhiev, O. Shabanov, A. Salikhova, A. Gadzhiev, S. Dzhamalova, G. Efendieva, High-voltage activation and dynamics of conductivity relaxation in a binary $\text{NaHSO}_4\text{-KHSO}_4$ system, *Russ. J. Electrochem* 45 (2) (2009) 215–220.
- [3] V.V. Martsinkevich, V.G. Ponomareva, Double salts $\text{Cs}_{1-x}\text{M}_x\text{H}_2\text{PO}_4$ ($\text{M} = \text{Na}, \text{K}, \text{Rb}$) as proton conductors, *Solid State Ionics* 225 (0) (2012) 236–240.
- [4] L. Korotkov, Proton ordering and spontaneous polarization in mixed KDP-ADP crystals, *Phys. Solid State* 43 (6) (2001) 1112–1116.
- [5] A.I. Baranov, V.V. Grebenev, A.N. Khodan, V.V. Dolbinina, E.P. Efreмова, Optimization of superprotonic acid salts for fuel cell applications, *Solid State Ionics* 176 (39–40) (2005) 2871–2874.
- [6] J. Otomo, N. Minagawa, C.-J. Wen, K. Eguchi, H. Takahashi, Protonic conduction of CsH_2PO_4 and its composite with silica in dry and humid atmospheres, *Solid State Ionics* 156 (3–4) (2003) 357–369.
- [7] V.G. Ponomareva, E.S. Shutova, High-temperature behavior of CsH_2PO_4 and $\text{CsH}_2\text{PO}_4\text{-SiO}_2$ composites, *Solid State Ionics* 178 (7–10) (2007) 729–734.
- [8] T. Matsui, T. Kukino, R. Kikuchi, K. Eguchi, An intermediate temperature proton-conducting electrolyte based on a $\text{CsH}_2\text{PO}_4/\text{SiP}_2\text{O}_7$ composite, *Electrochim. Solid-State Lett.* 8 (5) (2005) A256–A258.
- [9] Boysen D, Chisholm C, Haile SM, Uda T. Processing techniques for the fabrication of solid acid fuel cell membrane electrode assemblies. Google Patents; 2007.
- [10] S.M. Haile, C.R.I. Chisholm, K. Sasaki, D.A. Boysen, T. Uda, Solid acid proton conductors: from laboratory curiosities to fuel cell electrolytes, *Faraday Discuss.* 134 (2006) 17–39.
- [11] Taninouchi Y-k, T. Uda, Y. Awakura, A. Ikeda, S.M. Haile, Dehydration behavior of the superprotonic conductor CsH_2PO_4 at moderate temperatures: 230 to 260°C, *J. Mater. Chem.* 17 (30) (2007) 3182–3189.
- [12] C.E. Botez, J.D. Hermosillo, J. Zhang, J. Qian, Y. Zhao, J. Majzlan, et al., High-temperature phase transitions in CsH_2PO_4 under ambient and high-pressure conditions: a synchrotron x-ray diffraction study, *J. Chem. Phys.* 127 (19) (2007) 194701–194706.
- [13] A.I. Baranov, V.P. Khiznichenko, L.A. Shuvalov, High temperature phase transitions and proton conductivity in some kdp-family crystals, *Ferroelectrics* 100 (1) (1989) 135–141.
- [14] S. Hosseini, M. Homaiee, A.B. Mohamad, M.R. Malekbal, A.A.H. Khadum, Surfactant effect on the conductivity behavior of CsH_2PO_4 : characterization by electrochemical impedance spectroscopy, *Phys. B Condens. Matter* 406 (9) (2011) 1689–1694.
- [15] D.A. Boysen, S.M. Haile, H. Liu, R.A. Secco, High-temperature behavior of CsH_2PO_4 under both ambient and high pressure conditions, *Chem. Mater* 15 (3) (2003) 727–736.
- [16] B. Metcalfe, J.B. Clark, Differential scanning calorimetry of RbH_2PO_4 and CsH_2PO_4 , *Thermochim. Acta* 24 (1) (1978) 149–153.
- [17] N. Mohammad, A.B. Mohamad, A.A.H. Khadum, K.S. Loh, Conductivity and thermal stability of solid acid composites $\text{CsH}_2\text{PO}_4/\text{NaH}_2\text{PO}_4/\text{SiO}_2$, *Malays. J. Anal. Sci.* 20 (3) (2016) 633–641.
- [18] Z. Li, T. Tang, High-temperature thermal behaviors of XH_2PO_4 ($\text{X} = \text{Cs}, \text{Rb}, \text{K}, \text{Na}$) and LiH_2PO_3 , *Thermochim. Acta* 501 (1–2) (2010) 59–64.
- [19] L.C. Gupta, U.R.K. Rao, K.S. Venkateswarlu, B.R. Wani, Thermal stability of CsH_2PO_4 , *Thermochim. Acta* 42 (1) (1980) 85–90.
- [20] T.V. Anfimova, *Metal Phosphates as Proton Conducting Materials for Intermediate Temperature Fuel Cell and Electrolyser Applications* [PhD], Technical University of Denmark, 2014.
- [21] E. Ortiz, R.A. Vargas, B.E. Mellander, On the high-temperature phase transitions of CsH_2PO_4 : a polymorphic transition? *A. J. Chem. Phys.* 110 (10) (1999) 4847.
- [22] W. Bronowska, A. Pietraszko, X-ray study of the high-temperature phase transition of CsH_2PO_4 crystals, *Solid State Commun.* 76 (3) (1990) 293–298.
- [23] W. Bronowska, Comment on “Does the structural superionic phase transition at 231 °C in CsH_2PO_4 really not exist?” [*J. Chem. Phys.* 110, 4847 (1999)], *J. Chem. Phys.* 114 (1) (2001).